Mixture toxicity effects and uptake of titanium dioxide (TiO2) nanoparticles and 3,3,4,4-tetrachlorobiphenyl (PCB77) in juvenile brown trout following co-exposure via the diet

Lammel, Tobias; Wassmur, Britt; Mackevica, Aiga; Chen, Chang-Er L.; Sturve, Joachim

Published in:
Aquatic Toxicology

Link to article, DOI:
10.1016/j.aquatox.2019.04.021

Publication date:
2019

Document Version
Publisher's PDF, also known as Version of record

Aquatic Toxicology 213 (2019) 105195

Contents lists available at ScienceDirect

Aquatic Toxicology

journal homepage: www.elsevier.com/locate/aqtox

Mixture toxicity effects and uptake of titanium dioxide (TiO_2) nanoparticles and 3,3′,4,4′-tetrachlorobiphenyl (PCB77) in juvenile brown trout following co-exposure *via* the diet

Tobias Lammel[a,*], Britt Wassmur[a], Aiga Mackevica[d], Chang-Er L. Chen[b,c], Joachim Sturve[a]

[a] Department of Biological and Environmental Sciences, Gothenburg University, Sweden
[b] Department of Environmental Sciences and Analytical Chemistry, Stockholm University, Sweden
[c] Environmental Research Institute, South China Normal University, Guangzhou 510006, China
[d] TU Environment, Technical University of Denmark, Denmark

ARTICLE INFO

Keywords:
Nanomaterial
Metal oxide
Fish
Accumulation
Co-contaminant
Persistent organic pollutant

ABSTRACT

Titanium dioxide nanoparticles (n-TiO_2) are among the man-made nanomaterials that are predicted to be found at high concentrations in the aquatic environment. There, they likely co-exist with other chemical pollutants. Thus, n-TiO_2 and other chemical pollutants can be taken up together or accumulate independently from each other in prey organisms of fish. This can lead to dietary exposure of fish to n-TiO_2-chemical pollutant mixtures. In this study, we examine if simultaneous dietary exposure to n-TiO_2 and 3,3',4,4'-Tetrachlorobiphenyl (PCB77) –used as a model compound for persistent organic pollutants with dioxin-like properties– can influence the uptake and toxicological response elicited by the respective other substance. Juvenile brown trout (*Salmo trutta*) were fed custom-made food pellets containing n-TiO_2, PCB77 or n-TiO_2 + PCB77 mixtures for 15 days. Ti and PCB77 concentrations in the liver were measured by ICP-MS and GC–MS, respectively. Besides, n-TiO_2 uptake was assessed using TEM. Combination effects on endpoints specific for PCB77 (i.e., cytochrome P450 1A (CYP1A) induction) and endpoints shared by both PCB77 and n-TiO_2 (i.e., oxidative stress-related parameters) were measured in intestine and liver using RT-qPCR and enzyme activity assays. The results show that genes encoding for proteins/enzymes essential for tight junction function (*zo-1*) and ROS elimination (*sod-1*) were significantly upregulated in the intestine of fish exposed to n-TiO_2 and PCB77 mixtures, but not in the single-substance treatments. Besides, n-TiO_2 had a potentiating effect on PCB77-induced CYP1A and glutathione reductase (GR) expression/enzyme activity in the liver. This study shows that simultaneous dietary exposure to nanomaterials and traditional environmental pollutants might result in effects that are larger than observed for the substances alone, but that understanding the mechanistic basis of such effects remains challenging.

1. Introduction

Titanium dioxide nanoparticles (n-TiO_2) belong to the manufactured nanomaterials with the highest production volume and use in commercial and industrial products (Gottschalk et al., 2009; Hansen et al., 2016; Kaida et al., 2004; Piccinno et al., 2012; Schmid and Riediker, 2008). There is evidence that n-TiO_2 is released into the aquatic environment, that it can locally reach concentrations in the lower µg/L range in European surface waters, and that a significant proportion may settle out and accumulate in the sediment (Boxall et al., 2007; Brunelli et al., 2013; Coll et al., 2016; Gondikas et al., 2018; Gottschalk et al., 2011, 2009; Johnson et al., 2011; Kaegi et al., 2008; Peters et al., 2018; Praetorius et al., 2012; Slomberg et al., 2019). In the last years the scientific community has undertaken enormous efforts to assess the *innate* ecotoxic potential of n-TiO_2 (Menard et al., 2011), but there are comparatively few studies that have investigated their interaction and combined toxicological effects with co-existing "traditional" environmental pollutants (Canesi et al., 2015; Hartmann and Baun, 2010; Naasz et al., 2018). More information on this problem, especially the underlying mechanisms, is needed.

So far, most studies focussed on assessing combined effects between n-TiO_2 and inorganic co-contaminants (Naasz et al., 2018). These studies demonstrated that the co-existence of n-TiO_2 can enhance the uptake of heavy metals in different freshwater organisms (Canesi et al., 2015; Hartmann et al., 2012; Yang et al., 2014; Zhang et al., 2007). It is only recently that literature about combined effects between n-TiO_2 and

* Corresponding author.
E-mail address: tobias.lammel@gu.se (T. Lammel).

https://doi.org/10.1016/j.aquatox.2019.04.021
Received 22 December 2018; Received in revised form 10 April 2019; Accepted 29 April 2019
Available online 30 May 2019

persistent organic pollutants (POPs) such as organochlorinated compounds (e.g., dioxins, p,p'-dichlorodiphenyltrichloroethane (DDT), and polychlorinated biphenyls (PCBs)) started to emerge. That co-exposure to n-TiO_2 and PCBs may occur is a valid assumption. Both substances are likely to be present and co-exist in the aquatic environment. Furthermore, a recent study showed that some commercial n-TiO_2 powders may contain traces of PCBs that are formed during the fabrication processes (Ctistis et al., 2016), that is, both substances may enter the environment together. In vitro studies in human hepatocytes demonstrated that co-exposure to n-TiO_2 and DDT increases oxidative stress and DNA damage in a synergistic manner (Shi et al., 2010). Furthermore, n-TiO_2 and 2,3,7,8-tetrachlorodibenzo-p-dioxin (TCDD) were demonstrated to elicit both synergistic and antagonistic effects on various in vitro and in vivo toxicity endpoints in Mediterranean mussel (Canesi et al., 2014). There is also a growing body of literature reporting combined effects of n-TiO_2 and organic pollutants in aquatic vertebrates, specifically fish (Chen et al., 2018, 2019; Della Torre et al., 2015; Fang et al., 2016; Guo et al., 2019; Jhamtani et al., 2018; Qiang et al., 2016; Ren et al., 2018; Wang et al., 2014; Yan et al., 2014a, b). For instance, Della Torre et al. (2015) observed that waterborne co-exposure to n-TiO_2 and TCDD had antagonistic effects on TCDD-induced expression of immune response-associated genes and DNA damage in European sea bass. While waterborne exposure to NP-chemical[1] mixtures can occur, our current knowledge on the fate of nanomaterials and POPs in the aquatic environment suggests that dietary exposure may be more relevant.

It has been shown that n-TiO_2 and POPs end up in the sediment compartment, which makes it likely that they are taken up together and/or accumulate separately from each other in benthic invertebrates, which in turn may lead to intestinal exposure of predatory fish foraging on the former (Asztemborska et al., 2018; Kim et al., 2016; Maruya and Lee, 1998; Moermond et al., 2004; Van Geest et al., 2011; Wang et al., 2016). PCB concentrations in benthic invertebrates can reach significant levels. For instance, body burdens as high as ~1 mg/g lipid were reported in the oligochaete *Lumbriculus variegatum* exposed to field-contaminated sediment (Van Geest et al., 2011). Still little is known about n-TiO_2 uptake and accumulation in sediment-dwelling prey organisms of fish. A study in marine lugworm (*Arenicola marina*) showed that n-TiO_2 is ingested, but uptake from the gut lumen into the organism is limited (Galloway et al., 2010), which is largely consistent with findings in terrestrial soil organisms (Bigorgne et al., 2011; Hu et al., 2010; Lapied et al., 2011). However, fish will devour the entire prey organism including their gut content, that is, including sediment, where n-TiO_2 can reach concentrations in the lower mg/kg range (Gottschalk et al., 2009; Sun et al., 2014). n-TiO_2 accumulation in the gut was also observed in pelagic prey organisms of fish, for instance in Daphnia magnia, for which Ti body burdens up to 1 mg/g were reported after 24 h exposure to 1 mg/L (Zhu et al., 2010). It must also be noted that n-TiO_2 may adsorb to the outer surface of invertebrate prey organisms (Li et al., 2014) and that in marine fish dietary exposure may not only occur via the diet but also via drinking.

Previous studies showed that n-TiO_2 can cause injury to and cross the gut of fish (rainbow trout) (Al-Jubory and Handy, 2013; Federici et al., 2007). The molecular mechanisms underlying n-TiO_2 -induced intestinal injury and translocation in fish are unknown, but there are indications that n-TiO_2 exposure may deregulate tight junction protein expression leading to disruption of cellular tight junctions and increased paracellular permeability (Brun et al., 2014). Alteration of tight junction protein expression and gut permeability was also observed to occur upon exposure to PCBs (Choi et al., 2010). Based on these findings, we hypothesize that simultaneous exposure to n-TiO_2 and PCBs may have a combined adverse effect on intestinal barrier function facilitating their diffusion across the damaged epithelium. Besides, given their mutual capability to induce oxidative stress (Marabini et al., 2011; Schlezinger and Stegeman, 2001; Shi et al., 2013; Vignardi et al., 2015), we hypothesize that co-exposure to n-TiO_2 and PCBs may give rise to combined effects on this endpoint, which are larger than the effects caused by the individual substances alone. Moreover, it was suggested that the interaction of n-TiO_2 with PCBs may change their physicochemical properties and consequently kinetics in the organism (Schon et al., 2017).

The objective of this study was to examine if and how simultaneous dietary exposure to n-TiO_2 and PCB77 influences their fate and effect in juvenile brown trout focusing on intestine as the first site of interaction and important barrier for dietary toxicants and on liver as one of the key organs regarding xenobiotic accumulation, detoxification, and elimination.

2. Materials and methods

2.1. Chemicals

The test chemical[1] 3,3′,4,4′-tetrachlorobiphenyl (PCB77) was purchased from LGC Ltd. (Middlesex, United Kingdom). The surrogate standard 2,2′,5,5′- tetrachlorobiphenyl ($^{13}C_{12}$-PCB52) was purchased from Larodan AB (Solna, Sweden). 2,2´,5,6´-tetrachlorobiphenyl (PCB53) from AccuStandard was used as volumetric standard. Dimethylsulfoxide (DMSO), nicotinamide adenine di-nucleotide phosphate (reduced) (NADPH), 5,5′-Dithiobis(2-nitrobenzoic acid) (DTNB), 1-chloro-2,4-dinitrobenzene (CDNB), reduced and oxidized glutathione (GSH and GSSG), and ethylenediaminetetraacetic acid (EDTA) were obtained from Sigma-Aldrich. Acetone and n-hexane were obtained from Merck.

2.2. Nanomaterial

Nano-sized titanium dioxide (in the following abbreviated as n-TiO_2) was purchased as a powder from Sigma-Aldrich (Product number 718467; Synonym: Aeroxide® P25, Titania, Titanium (IV) oxide). The primary particle size (TEM), surface area (BET) and purity (trace metals basis) indicated by the manufacturer was 21 nm, 35–65 m^2/g, and ≥99.5%, respectively. Own characterization data including the primary particle size-frequency distribution and shape descriptors of the NPs were described previously in detail (Lammel and Sturve, 2018).

2.3. Preparation of test diets

First, aqueous NP dispersions (0.1 and 1 mg/ml n-TiO_2 /Milli-Q water) were prepared using the ultrasonication protocol specified in Lammel and Sturve (2018). The dispersions' characteristics were determined by means of dynamic light scattering (DLS) and phase analysis light scattering (PALS) analysis and were described in detail in the aforementioned paper. In brief, the n-TiO_2 dispersions had a monomodal size-intensity distribution with a z-average of 160.8 ± 2.6 nm (mean diameter ± SD; n = 3), which did not change with time. The zeta-potential was 26.6 ± 5.0 mV. Following their preparation, the NP dispersions (0.1 and 1 mg/ml n-TiO_2 /Milli-Q water) were spiked with PCB77 (dissolved in DMSO) yielding two different NP-chemical[1] mixtures: 1 mg/ml n-TiO_2 + 10 µg/ml PCB77 and 0.1 mg/ml n-TiO_2 + 10 µg/ml PCB77. A 10 µg/ml PCB77 solution in Milli-Q water was prepared as chemical only control. In parallel, NP dispersions and Milli-Q water were spiked with only DMSO (not containing any PCB) yielding the corresponding n-TiO_2 only solutions and the solvent control (1 mg/ml n-TiO_2 + 1% DMSO, 0.1 mg/ml n-TiO_2 + 1% DMSO and 1% DMSO only, respectively). Thereafter, commercially available fish food in flake form (NovoBel, JBL GmbH & Co.KG, Neuhofen, Germany) was added to

[1] In this article, the authors use the term" chemical" to refer to non-particulate substances, as opposed to the terms "nanomaterial" and"nanoparticle", which are used to refer to particulate substances with dimensions in the nanometric range.

each dispersion/solution and the soaked flakes were macerated and mixed using a stainless steel spoon until full homogeneity of the food paste was achieved. Subsequently, gelatin (Dr Oetker Sverige AB, Sweden) was added and intermixed with the food paste (final concentration 5% w/w) in order to improve its consistency and viscoelastic properties. The food paste was filled into disposable syringes and then extruded through their tip yielding 2 mm-thick "food worms", which were then left to dry at room temperature and after that cut into small pellets of similar size.

2.4. Fish husbandry

Brown trout (*Salmo trutta*) fry were obtained from a local hatchery and kept in a large-volume holding tank in aerated, 10 °C-cold, dechlorinated tap water supplied via the in-house semi-circulating system. The light/dark cycle was 12 h/12 h. Fish were fed commercial food pellets on a maintenance food ration (˜2% of their average body wet weight (ww) per day).

2.5. Dietary exposure and sampling

One week prior to exposure start 48 fish (average body ww: ˜ 10 g) were captured from the holding tank and transferred to separate polypropylene tanks (1.5 L) of an experimental flow-through system, each equipped with an air stone and supplied with water (10 °C; flow ˜ 6 L/h) from the in-house semi-circulating system. The tanks were assigned to the different treatment groups in such way that potential effects by extraneous factors (proximity to walkway, proximity to light source, etc.) would carry similar weight (systematic randomization). In total, the study comprised six treatment groups at eight fish each. Fish were kept and exposed singly in separate tanks, that is, each tank/fish represented a true replicate (n = 8). The average body ww of fish in the different treatment groups was similar (10.6 ± 1.4 g; 10.3 ± 1.0 g, 10.6 ± 1.5 g, 10.4 ± 1.5 g, 9.6 ± 0.9 g, 10.3 ± 2.1 g). The fish were fed custom-made pellets (see above) containing n-TiO_2 alone, PCB77 alone, n-TiO_2 – PCB77 mixtures or no test substance (negative control) for 15 days (prior to exposure start feeding was suspended for two days). Each fish received ˜750 mg test diet in total, administered as evenly distributed daily rations of ˜50 mg (≙ 0.5% of the fishes' average body ww at beginning of exposure). The dietary exposure doses per g fish body ww per day were: 1 µg n-TiO_2, 10 µg n-TiO_2 (single NP exposures), 0.01 µg PCB77 (single chemical exposure), and 1 µg n-TiO_2 + 0.01 µg PCB77, 10 µg n-TiO_2 + 0.01 µg PCB77 (NP-chemical mixture exposures). Fish in the control group were fed pellets, which only contained the solvent (0.1% DMSO). All fish were treated in accordance with the ethical practices defined by the Swedish Board of Agriculture (Permit number: 220–2013).

At the end of experimental day 15, fish were killed with a sharp blow to the head. Following determination of body ww and length, blood was collected by caudal puncture and organs including liver and intestine were excised. Livers and intestine were sectioned into four pieces (perpendicular to the anteroposterior axis) for the different chemical and biological analyses, snap-frozen in liquid nitrogen and stored at -80 C. In addition, from fish exposed to the highest n-TiO_2 dose, tissue pieces were fixed for transmission electron microscopy (TEM) analysis.

2.6. Calculation of condition factor and liver somatic index

The Fulton's condition factor (K) and liver somatic index (LSI) were determined to obtain additional information on possible treatment-dependent differences in feeding, assimilation and energy expenditure as well as the general health condition of the fish. The Fulton's condition factor was calculated as K = $(ww/l^3)*100$. The LSI was expressed as percentage liver weight of total body ww.

2.7. Staining and counting of blood cells

Brown trout blood smears were prepared, fixed in methanol and after that stained with May-Grünwald and Giemsa solution. Then, images were taken using a microscope (Leitz Biomed) and the number of thrombocytes, red blood cells and white blood cells (granulocytes, lymphocytes, and monocytes) counted using ImageJ software version:2.0.0-rc-68/1.52i (National Institutes of Health, USA; http://imagej.nih.gov/ij), whereas a minimum of 500 cells was counted per slide (i.e., fish).

2.8. Transmission electron microscopy analysis

TEM analysis was only performed on tissues of fish exposed to the highest n-TiO_2 dose. Liver samples were taken from the central region of the organ in proximity to the entry of the hepatic portal vein. Intestine samples were taken from the proximal end of the excised intestinal tract (˜1-5 mm posterior of the pyloric ceca). They were cut open along the luminal cavity and gently flushed with ice-cold PBS to remove chyme/feces. Liver and intestine samples were fixed in ice-cold modified Karnovsky fixative (2.5% glutaraldehyde, 2% paraformaldehyde, 0.05 M Na-cacodylate, 0.02% Na-azide) for 4 h and stored in a 1:10 dilution of the fixative in 0.05 M cacodylate buffer (pH 7.4) until start of dehydration (˜48 h). Samples were post-fixed in 1% OsO_4 in Na-cacodylate at 4 C for 2 h, after that washed 3 x 5 min with distilled H_2O and then stained "en bloc" with 0.5% uranyl acetate (in distilled H_2O) in the dark for 1 h. The samples were dehydrated in a graded series of EtOH (2 x 5 min 70%, 1 x 5 min 85%, 1 x 5 min 95%, 4 × 5 min 100%) followed by incubation in 100% acetone (3 x 15 min), and gradually infiltrated and embedded in Agar 100 resin (Agar Scientific Ltd., United Kingdom). Resin blocks were cut with a Leica UC60 ultramicrotome. Ultrathin sections (˜70 nm) were collected on copper grids and counterstained with uranyl acetate and Reynolds' lead citrate (Agar Scientific Ltd.). Sections were analyzed with a Zeiss Leo 178 912 AB transmission electron microscope (Zeiss, Germany) operated at 120 kV. Digital images were recorded with a Veleta CCD camera.

2.9. Molecular biology analysis

Tissue samples were homogenized using stainless steel beads (5 mm, Quiagen) and a TissueLyser II apparatus (Qiagen). Total RNA was isolated using the RNeasy Plus Mini Kit from Quiagen. RNA concentration and purity were measured on a NanoDrop 2000c spectrophotometer (ThermoFisher). cDNA was synthesized using the iScript™ cDNA synthesis kit from BioRad. Quantitative polymerase chain reaction (qPCR) was performed using the primers specified in Table 1, SsoAdvanced™ Universal SYBR Green Supermix and the CFX Connect™ Real-Time System from Bio-Rad. The primer concentration in the qPCR assay was 500 nM. All reactions were run in duplicate using the following program: 1 x 3 min at 95 °C followed by 40 × 10 s at 95 °C and 30 s at 60 °C. No-RT controls (=no reverse transcriptase added during cDNA synthesis step) were included to control for genomic DNA contamination. NTC controls (=no template controls) were included to control for random or reagent contamination as well as primer dimer formation.

ΔCq values were calculated subtracting the Cq value (mean of duplicates) of each target gene by the Cq values (mean of duplicates) of the reference gene. Fold change (FC) expression levels were calculated as $FC = 2^{-\Delta\Delta Cq}$, whereas ΔΔCq = ΔCq (negative control) - ΔCq (treatment).The corresponding upper and lower bound were calculated as $FC_{max} = 2^{-\Delta\Delta Cq\text{-}SD}$ and $FC_{min} = 2^{-\Delta\Delta Cq + SD}$. Statistical comparisons of gene expression levels were carried out on ΔCq values (see below for further details).

2.10. Biochemical analysis

Tissue samples were homogenized in 0.1 M Na-K-phosphate buffer

Table 1
Primer sequences used for qPCR.

Gene	Acc. no.	Sequence (5'- > 3') of forward (fw) and reverse (rv) primers		Ref.
18S rRNA (*18S*)	AJ427629	fw	CCCCGTAATTGGAATGAGTACACTTT	(Hansen et al., 2007a)
		rv	ACGCTATTGGAGCTGGAATTACC	
Tight junction protein 1a (*zo-1*)	HQ656020	fw	AAGGAAGGTCTGGAGGAAGG	(Kelly and Chasiotis, 2011)
		rv	CAGCTTGCCGTTGTAGAGG	
Claudin-12 (*cldn-12*)	BK007967	fw	CTTCATCATCGCCTTCATCTC	(Kelly and Chasiotis, 2011)
		rv	GAGCCAAACAGTAGCCCAGTAG	
Metallothionein-A (*mta*)	X97274	fw	CCTTGTGAATGCTCCAAAACTG	(Hansen et al., 2007b)
		rv	CAGTCGCAGCAACTTGCTTTC	
Gluathione reductase (*gr*)	BG934480	fw	CCAGTGATGGCTTTTTTGAACTT	(Hansen et al., 2007b)
		rv	CCGGCCCCCACTATGAC	
Glutathione peroxidase (*gpx*)	BG934453	fw	GATTCGTTCCAAACTTCCTGCTA	(Hansen et al., 2007b)
		rv	GCTCCCAGAACAGCCTGTTG	
Superoxide dismutase-1 (*sod-1*)	BG936553	fw	CCACGTCCATGCCTTTGG	(Hansen et al., 2007b)
		rv	TCAGCTGCTGCAGTCACGTT	
Cytochrome p450 1A (*cyp1a*)	AF539415	fw	CCAAACTTACCTCTGCTGGAAGC	(Meland et al., 2010)
		rv	GGTGAACGGCAGGAAGGA	

(pH 7.5) by application of ultrasound pulses while being incubated in an ice-cold water bath. Subsequently, the homogenates were centrifuged at 10,000 x g for 20 min at 4 °C, and the supernatant (S9 fraction) was collected, aliquoted and stored frozen at -80 °C until biochemical analysis.

CYP1A-dependent ethoxyresorufin-O-deethylase (EROD) activity was measured in the S9 fraction using the method described by Forlin et al. (1984) (Forlin et al., 1984). In brief, samples were diluted in 0.1 M sodium phosphate buffer (pH 8) containing 2.5 µM 7-ethoxyresorufin and 0.05 mM NADPH and thereafter the increase in resorufin fluorescence was monitored over time on a fluorescence spectrometer using 530 nm and 585 nm as excitation and emission wavelength, respectively. The total protein content in samples was determined according to (Lowry et al., 1951).

Glutathione reductase (GR) activity was measured using the method described by Cribb et al. (1989) (Cribb et al., 1989). First, samples were diluted in 0.1 M sodium phosphate buffer (pH 7.5) containing EDTA (1 mM), NADPH, and DTNB. Then, the reaction was initiated by adding GSSG (concentration in the assay: 0.25 mg/ml) and the increase in absorbance was measured at 415 nm in a Spectra Max 190 microplate spectrophotometer.

Glutathione S-Transferase (GST) enzyme activity was measured as described by Habig et al. (1974) adapted to a microplate reader as described in Stephensen et al. (2002) (Habig et al., 1974; Stephensen et al., 2002). In brief, samples were diluted in 0.1 M sodium phosphate buffer (pH 7.5) containing 2 mM CDNB and 1 mM GSH, and the absorbance was measured at 350 nm in a Spectra Max 190 microplate spectrophotometer.

Catalase (CAT) enzyme activity was measured according to the method described by Aebi (1984) and modified by Sturve et al. (2005) to be used with a microplate reader (Aebi, 1984; Sturve et al., 2005). In brief, samples were diluted in 0.08 M KPO_4-buffer pH 6.5 followed by addition of 0.08 M H_2O_2 as substrate. The rate of H_2O_2 consumption was determined measuring the decline in absorbance at 240 nm in a Spectra Max 190 microplate spectrophotometer.

2.11. Chemical analysis

2.11.1. PCB77 extraction and GC–MS analysis

Sample preparation for extraction of PCB77 in fish tissues generally followed the method by Pena-Abaurrea et al. (2013) with some modifications (Pena-Abaurrea et al., 2013). Briefly, the liver and food pellet homogenates were spiked with 10 ng surrogate standard $13C_{12}$-PCB52. Then, 10 mL 1/1 (v/v) n-hexane/acetone was added and the samples placed in an ultrasound bath for 15 min. Subsequently, the samples were centrifuged at 3000 rpm for 5 min and the supernatant transferred to a glass vial. The procedure (ultrasound assisted extraction) was repeated two more times, the first time with 1/1 (v/v) n-hexane/acetone and the second time with pure n-hexane. The organic phases obtained via centrifugation were pooled and left to dry under a stream of N_2 gas. The extract was reconstituted in 1 mL n-hexane and then loaded onto acid silica columns for clean-up (10 mL SPE columns containing three consecutive layers of 1 g Na_2SO_4, 3 g acid silica, 1 g Na_2SO_4, washed with 20 mL n-hexane). Following elution with 10 mL n-hexane/dichloromethane(7/3, v/v), the solvent was evaporated under N_2 until about 100 µL, which were then transferred to GC vials. The vials were sealed and stored at 4 °C until analysis. The above procedure was evaluated by spiking PCB77 at 0.5 ng/g and 5 ng/g levels to fish tissue (ww) which gave recoveries of 94% and 101%, respectively.

The samples were spiked with 10 ng of volumetric standard (PCB53) before instrumental analysis. Sample analysis was performed using a Trace 1300 Series gas chromatograph (GC) (Thermo Scientific) equipped with a programmed temperature vaporizing (PTV) injector and an AI 1310 Autosampler (Thermo Scientific), coupled to a single quadrupole ISQ mass spectrophotometer (MS) (Thermo Scientific). The PTV injector was run in splitless mode (1.5 min), and the temperature started at 60 °C, was held constant for 0.5 min, increased by 14.5 °C/s to 300 °C, where it was held constant for 1 min. A Thermo TG-5SIL MS capillary column (30 m × 0.25 mm i.d., 0.25 µm film) was used with helium (at a constant flow 1 mL/min) as the carrier gas. The oven temperature started at 60 °C, was held constant for 2 min, increased by 10 °C/min to 250 °C and then by 30 °C/min to 300 °C, where it was held constant for 2 min. The transfer line was set to 300 °C and the ion source to 260 °C. The MS instrument was operated in electron ionization (EI) mode (70 eV), and selective ion monitoring (SIM) mode for scanning for ions of target compounds with a dwelling time of 0.01 s each. The internal standard method was employed to quantify the target chemicals in the samples. A ten points calibration solutions (0.1 ng/mL – 500 ng/mL) was prepared and used to quantify PCB77 with a regression coefficient $R^2 > 0.99$. The method detection limit (MDL) based on the blanks was 0.3 ng/g (ww).

2.11.2. ICP-MS analysis

The total content of titanium in liver samples was analyzed by ICP-MS (PerkinElmer, NexION 350D), following microwave-assisted acid digestion (Multiwave 3000, Anton-Paar). Liver samples were pooled in groups of 3 or 4 livers per sample. Microwave-assisted acid digestion was performed by adding 5 mL of HNO_3 (65%, Suprapure, Merck) and 1 mL of HF (40%, Suprapure, Merck), and microwaving at 1400 W for 15 min. After digestion, 6 mL of H_3BrO_3 (10%, Suprapure, Sigma Aldrich) were added for HF complexation, and samples were again microwaved at 600 W for 15 min. Thereafter, samples were diluted with deionized water (Merck KGaA, Milli-Q) and analyzed using ICP-MS. The recovery by using the above digestion method was 105 ± 1% (n = 3)

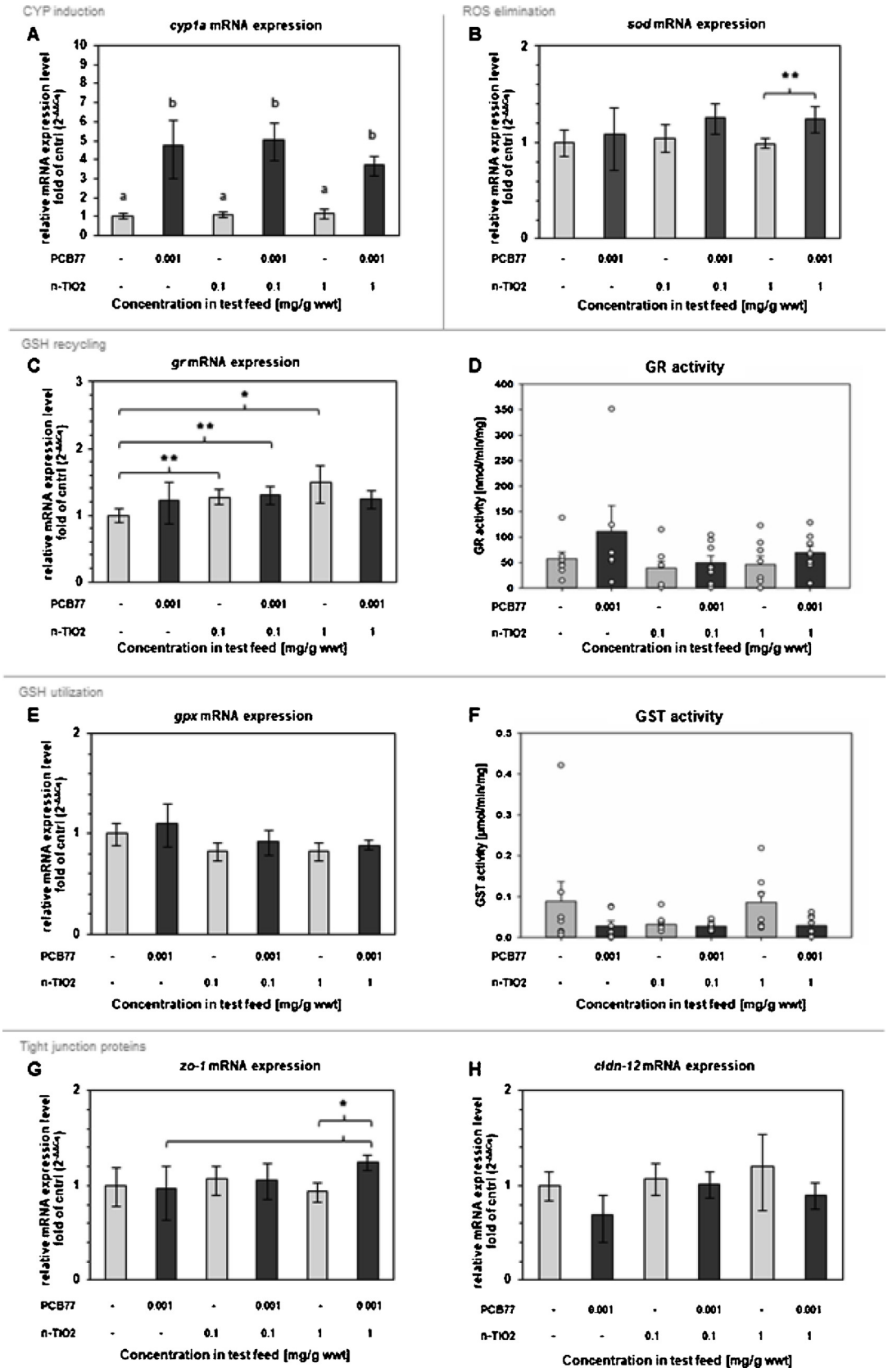

Fig. 1. Combined effects on gene expression and enzyme activities in intestines of brown trout exposed to n-TiO_2, PCB77 and n-TiO_2 + PCB77 containing food. Bars in graphs showing mRNA expression levels (A, B, C, E, G and H) show the mean fold change with respect to the negative control (-/-). Error bars in these graphs show the lower and upper bound calculated from the standard error (SE) of $\Delta\Delta C_q$ values (n = 7–8). Bars and error bars in graphs showing results of enzymatic assays (D and F) represent the mean specific enzyme activity and its standard error (SE) (n = 6–8). The open circles (○) in the graphs show the enzyme activities measured in each fish (here included to better illustrate inter-individual variability). Bars/treatment groups that do not share the same letter were significantly different from each other when compared using One Way ANOVA or a corresponding non-parametric test. Significant differences detected between two treatment groups using a *t*-test, or a corresponding non-parametric test, are indicated by curly brackets and asterisks (*$p < 0.05$, **$p < 0.01$).

using suspensions of 30–50 nm TiO_2 nanoparticles (US Research Nanomaterials Houston, Texas, USA). The IDL (instrument detection limit), that is, the lowest measurable calibration point was 0.10 µg/L. The MDL (method detection limit), defined as blank average + 3x SD, based on blank samples from acid digestion (n = 6) was 0.529 µg/L.

2.11.3. Statistical analysis

Statistical comparisons between multiple treatments were carried out using One Way Analysis of Variance (One-way ANOVA) followed by an appropriate posthoc test (Student-Newman-Keuls Method). When the data did not meet the requirements for the use of a parametric statistical test (i.e., normality and homoscedasticity), a non-parametric statistical test, specifically Kruskal-Wallis One Way ANOVA on Ranks was used for all pairwise comparisons. In addition, selected pairs of treatment groups were compared using a *t*-test or Mann-Whitney Rank Sum Test. All statistical tests were performed using SigmaPlot for Windows Version 13.0 (Systat Software, Inc.).

3. Results

3.1. Nanoparticle characterization and test diet preparation

The n-TiO_2 stock dispersion used for test diet spiking has been extensively characterized. Data on the hydrodynamic size distribution, zeta-potential, long-term stability and accuracy when performing serial dilutions, etc. are described in detail in Lammel and Sturve (2018) (Lammel and Sturve, 2018). A representative TEM image of the NPs in the stock dispersion has been included in Figure A. ***1*** in the appendix (as well as in Fig. 5 in order to allow direct comparison with NP-resembling electron dense-objects identified in TEM images of tissue sections; see below).

The PCB77 concentration measured in NP-free diet corresponded to the nominal concentration (1.028 vs. 1.000 µg/g food ww, respectively). The PCB77 concentration measured in 0.1 and 1 mg/g NP-containing diet, however, was considerably lower (0.705 and 0.275 µg/g food ww, respectively) and inversely related with the n-TiO_2 concentration in the diet. This suggests that the presence of n-TiO_2 affected the efficiency with which PCB77 could be extracted from food –possibly by binding a fraction of the chemical to its surface. This is an important observation, as the binding of PCB77 to n-TiO_2 is likely to influence its availability for intestinal uptake.

3.2. Food intake and fish health

The fish generally consumed the prepared test diet with high-efficiency. Occasionally some fish did not consume the food pellets. These food pellets were removed from the tank. The amount of food consumed by each fish is shown together with the corresponding exposure doses in Table A1 in the appendix. No statistically significant differences in food intake were observed between treatment groups (Kruskal-Wallis One Way ANOVA on Ranks). Furthermore, no differences in fish growth, indirect indices of energy status (K, LSI), and white blood cell ratio were observed (Table A2) (Kruskal-Wallis One Way ANOVA on Ranks).

3.3. Combined toxicological effects of dietborne n-TiO_2 and PCB77

3.3.1. Biomarker responses in intestinal tissue

All fish receiving test diet containing 0.001 mg PCB77/g food ww showed significantly increased intestinal *cyp1a* mRNA levels ($p < 0.001$, One Way ANOVA followed by Holm-Sidak method). A slight decrease in PCB-induced *cyp1a* expression was observed in the treatment where n-TiO_2 was simultaneously present (at 1 mg/g food ww), but it was not statistically significant compared to the PCB-only control. Dietary exposure to n-TiO_2 alone did not induce intestinal *cyp1a* mRNA expression. CYP1A-dependent EROD activity could not be measured in intestinal samples.

For *sod-1* a similar pattern was observed as for *cyp1a*. Transcript levels seemed to be slightly elevated in the intestine of all fish fed PCB77-containing diet but were only significantly different from control levels in the mixture treatment with the highest n-TiO_2 concentration. Fish fed diet containing only n-TiO_2 did not demonstrate any changes in *sod-1* expression compared to control fish (Fig. 1B).

GR was observed to be significantly upregulated in all fish exposed to n-TiO_2-containing food when separately compared to the control (control vs. 0.1 mg n-TiO2, control vs. 1 mg n-TiO2, *t*-test, $p < 0.01$; control vs. 0.1 mg n-TiO2 + PCB77, Mann-Whitney Rank Sum Test, $p < 0.05$), except in the highest mixture treatment (1 mg n-TiO2 + 0.001 mg PCB77/g food ww) (Fig. 1C). All pair-wise comparison using ANOVA did not indicate any statistically significant differences, and effects did not manifest at the enzyme activity level (GR) (Fig. 1D). For the other two glutathione system-related parameters analyzed in the intestine, *gpx* and GST, no significant differences or indications for combined effects could be observed (Fig. 1E and F). However, there seemed to be a consistent trend towards *gpx* mRNA levels being slightly elevated following dietary exposure to PCB77-containing food (including mixtures) compared to the corresponding controls (treatments without PCB77) (Fig. 1E).

Interestingly, as hypothesized, for one of the two tight junction protein-encoding genes (*zo-1*) a combined effect was observed. While dietary exposure to PCB77 or n-TiO_2 (1 mg/g food ww) alone did not have any effect on *zo-1* expression, in the corresponding mixture treatment a statistically significant upregulation was detected (*t*-test, $p < 0.05$) (Fig. 1G). Intestinal *cldn-12* expression was not significantly altered in any of the exposures (Fig. 1H).

3.3.2. Biomarker responses in hepatic tissues

All fish receiving test diet containing 0.001 mg PCB77/g ww food (corresponding to a daily dose of 10 ng PCB77/g body ww) had significantly increased hepatic *cyp1a* mRNA levels and CYP1A enzymatic activity. Furthermore, the simultaneous presence of n-TiO_2 in the test diet resulted in an additional increase of CYP1A levels. A clear positive trend could be seen at the transcriptional level (Fig. 2A). In addition, a statistically significant difference in the mean EROD activity of mixture-exposed fish (0.001 mg PCB77 + 1 mg n-TiO_2 /g food ww) and PCB-only exposed fish (0.001 mg PCB77/g food ww) was observed (Kruskal-Wallis One Way ANOVA on Ranks, $p = 0.026$) (Fig. 2B). Interestingly, dietborne exposure to the nanomaterial alone also resulted in statistically significant upregulation of *cyp1a* transcription (solvent control vs. 0.1 mg n-TiO_2 /g ww food: $p = 0.013$; solvent control vs. 1 mg n-TiO_2 /g ww food: $p = 0.032$; One Way ANOVA followed by all pairwise comparison according to Student-Newman-Keuls Method, $n = 8$) (Fig. 2A). However, this effect did not manifest itself at the enzyme activity level.

Furthermore, genes and enzymes involved in the elimination of reactive oxygen species (ROS), namely superoxide dismutase and catalase were found to be slightly downregulated in liver of brown trout that received test diet containing PCB77, except when n-TiO_2 was additionally present at 1 mg/g in the food, where an increase was observed (Fig. 3A and B). One Way ANOVA did not indicate any statistically significant differences between means, but one-to-one comparison of selected treatment groups using a *t*-test (or where not applicable a non-parametric test) did. Note that the effect level patterns in Fig. 3A and B are congruent, despite the fact that *sod-1* expression was measured at the transcriptional and CAT expression at the catalytic activity level.

The hepatic GR induction pattern resembled that observed for CYP1A (though effect levels were generally lower). Dietborne exposure to the organic chemical alone resulted in a statistically significant induction of GR. Furthermore, a clear trend towards increased GR expression with increasing n-TiO_2 concentration in the test diet was observed (Fig. 3C and D). The differences in GR enzyme activity between

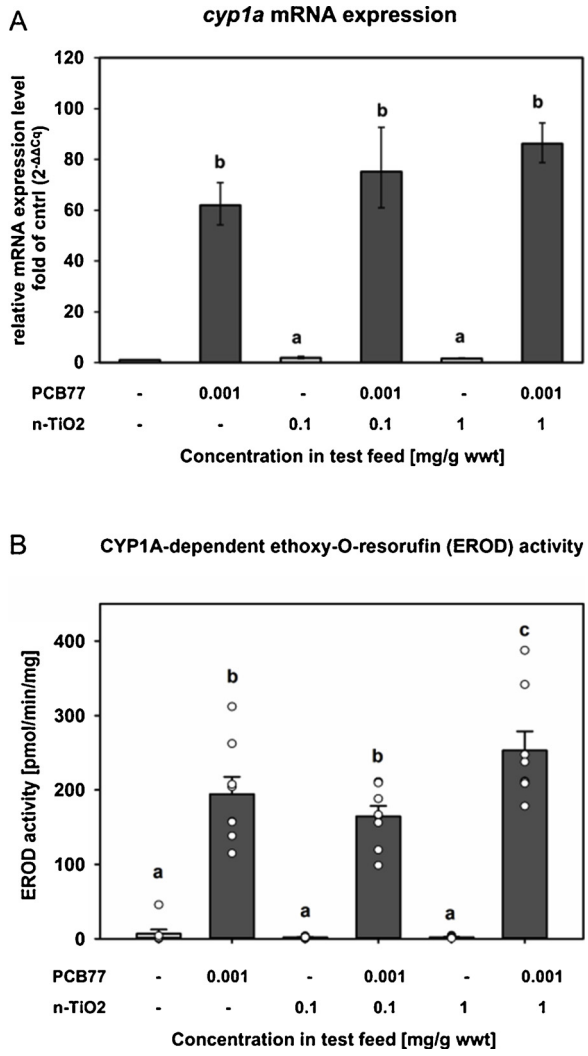

Fig. 2. *CYP1A* mRNA expression and EROD activity levels in liver of brown trout following dietary exposure to n-TiO2, PCB77, and n-TiO2 + PCB77. Bars in A show the mean fold change in gene expression level with respect to the negative control (-/-). Error bars show the lower and upper bound calculated from the standard error (SE) of $\Delta\Delta C_q$ values (n = 8). Bars and error bars in B show the mean EROD activity and its standard error (SE) in liver of eight singly exposed fish (n = 8). Open circles (○) show hepatic EROD activities measured in each individual fish, which were presented in addition to the mean values to better illustrate inter-individual variability. Bars that do not share the same letter indicate statistically significant differences between treatment groups.

the n-TiO_2/PCB77-mixture and PCB77-only exposure were statistically significant (0.001 mg PCB77 + 1 mg n-TiO vs. 0.001 mg PCB77/g ww food: $p < 0.001$; and 0.001 mg PCB77 + 1 mg n-TiO_2 vs. 0.001 mg PCB77 + 0.1 mg n-TiO_2/g ww food: $p < 0.001$; Kruskal-Wallis One Way ANOVA on Ranks followed by Student-Newman-Keuls Method). In addition, the GR induction levels in the mixture-treatments were greater than the sum of the GR induction levels measured in the corresponding single substance-treatments. In fact, no GR induction was observed for fish that had received diet containing only the nanomaterial. This suggests that the presence of n-TiO_2 in the mixture treatment (n-TiO_2 and PCB77 co-contaminated diet) had a potentiating effect on PCB77-induced GR expression/activity. Also, note that the inter-replicate variability in GR enzyme activity levels increased when n-TiO_2 was present as a co-contaminant in the food.

Concomitant with the increase in GR expression and activity, a significantly elevated expression of the gene encoding for the glutathione-utilizing enzyme GPx was observed (Fig. 3E). However, opposed to GR and CYP1A, no n-TiO_2 concentration-dependent trend, that is, combined toxicological effect was observed.

Mean GST activity levels were found to be comparable among all treatment groups except for the mixture exposure with the highest n-TiO_2concentration (0.001 mg PCB77 + 1 mg n-TiO_2/g ww food), for which an obvious, albeit statistically not significant increase was observed (Fig. 3F).

3.4. Dietary uptake and accumulation of n-TiO_2 and PCB77 in the liver

3.4.1. Location of n-TiO_2 in the liver

Fig. 4 shows a TEM image of an ultrathin section of the liver of a brown trout that received diet containing only n-TiO_2 and no PCB77 (dietary exposure dose: 10 µg n-TiO_2/g bw/day; exposure duration: 15 days). An electron-dense object was identified in the space of Disse (= perisinusoidal space) (Fig. 4A). Fig. 4B, showing the boxed-in area at higher magnification, demonstrates that the object physically interacted with microvilli of hepatocytes extending into the perisinusoidal space. Both the size (˜100 nm) and morphology of this object (three-dimensionally ramified structure composed of several small entities) strongly resembled the n-TiO_2 agglomerates in the stock dispersion that was used for spiking of the test diet (Figure A. 1). What is more, the size of the individual entities matched the primary particle size of the n-TiO_2 used in this study (Aeroxide® P25) (compare Fig. 4B and Fig. 4C) (Note that electron-dense particulate objects were also seen in the intestine, but their morphology was less similar to n-TiO_2, Figure A. 2).

3.4.2. Effects on biomarkers of metal exposure: metallothionein induction

Metallothionein was measured as a biomarker of metal exposure. Indeed, fish receiving n-TiO_2-spiked diet demonstrated elevated hepatic metallothionein-A (mta) mRNA expression levels (Fig. 5). For instance, in fish receiving pellets containing 0.1 and 1 mg n-TiO_2 per g food ww (corresponding to an average dietborne dose of 1 and 10 µg n-TiO_2 per day and g fish) they were ˜1.4-fold higher than in control fish. However, no statistically significant differences were detected between the corresponding Cq-value means (Kruskal-Wallis One Way ANOVA on Ranks, $p = 0.311$, $n = 8$). Interestingly, mta mRNA expression levels in fish fed with pellets containing 1 mg n-TiO_2 and 0.001 mg PCB77 per g ww food (corresponding to 10 µg n-TiO_2 and 10 ng PCB77 per day per and g fish) were ˜1.7-fold increased with respect to the solvent control. Furthermore, the Cq-value mean of this treatment group exceeded the Cq-value mean of the PCB77 control by an amount that is greater than would be expected by chance (t-test, $p = 0.045$, $n = 8$) suggesting a combined effect on this endpoint.

3.4.3. Ti and PCB77 levels in the liver

The average Ti content in the liver of fish exposed to the highest n-TiO_2 dose was slightly higher than in fish receiving control diet (0.334 ± 0.129 vs. 0.264 ± 0.019 µg Ti/g liver ww, respectively), but the Ti content of all samples was below the MDL (= 0.529 µg/L) (Table A ***3***), that is, below the lowest Ti concentration that can be distinguished with 99% confidence from the blank. This indicates that there was no (at least no detectable) n-TiO_2 uptake into hepatic tissue.

However, the simultaneous presence of n-TiO_2 in the food appeared to influence PCB77 availability and accumulation in liver. While, in the PCB77-only treatment merely two out of eight samples had PCB77 levels above the MDL (= 0.3 ng/g tissue ww), in the PCB77 + n-TiO_2 treatments four out of eight samples could be measured. Furthermore, fish fed test diet spiked with n-TiO_2-PCB77 mixtures had a higher hepatic PCB77 concentration than fish that received test diet containing only the chemical (on average). Also, a n-TiO_2-dependent trend was observed: The higher the concentration of the nanoparticulate co-contaminant in the test diet, the higher the amount of PCB77 measured in the liver (Table 2). However, the differences were not statistically significant (Kruskal-Wallis One Way ANOVA on Ranks, $p = 0.671$).

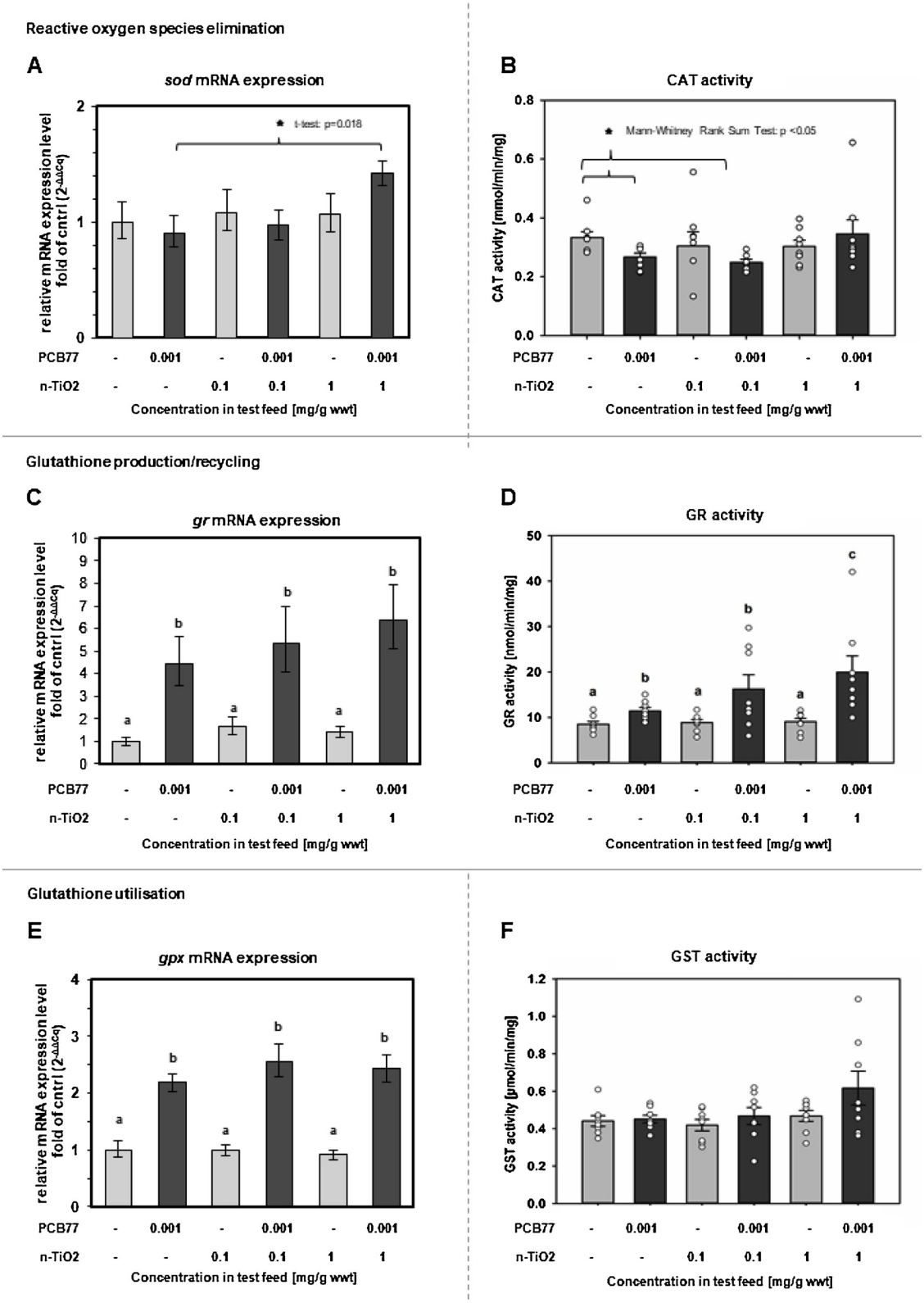

Fig. 3. Combined effects on oxidative stress-related biomarkers in liver of brown trout exposed to n-TiO2, PCB77 and n-TiO2 + PCB77 containing food. Bars in graphs showing mRNA expression levels (A, C and E) represent the mean fold change with respect to the negative control (-/-). Error bars in these graphs show the lower and upper bound calculated from the standard error (SE) of $\Delta\Delta C_q$ values (n = 8). Bars and error bars in graphs showing results of enzymatic assays (B, D, and F) represent the mean specific enzyme activity and its standard error (SE) (n = 8). The open circles (○) in the graphs show the enzyme activities measured in each fish (here included to better illustrate inter-individual variability). Bars/treatment groups that do not share the same letter were significantly different from each other in all pairwise comparisons (ANOVA). Significant differences detected comparing two treatment groups. Significant differences detected comparing two treatment groups with each other (denoted by braces) are indicated by asterisks (Graph A: *p < 0.05, *t*-test; Graph B: *p < 0.05 Mann-Whitney Rank Sum Test).

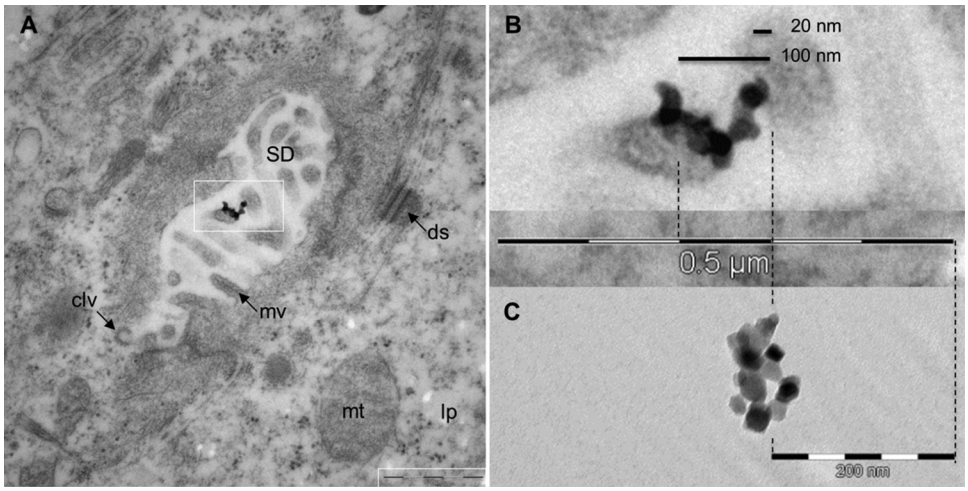

Fig. 4. TEM image of brown trout liver section. A. Electron-dense object resembling n-TiO_2 located in the Space of Disse of a sinusoid in liver of brown trout exposed to diet with the highest n-TiO_2 concentration. SD = Space of Disse (perisinusoidal space), mv = microvilli of hepatocytes, ds = desmosomes connecting adjacent hepatocytes, clv = clathrin-coated vesicle, mt = mitochondrion, lp = lipid vesicles. The scale bar in A corresponds to 0.5 µm. The boxed-in areas in A were cropped and are shown together as amplified composite image in B. C. n-TiO_2 agglomerate in stock dispersion used for food spiking. The scale bar in C correspond to 200 nm. Dotted lines were inserted to facilitate comparison of particle sizes.

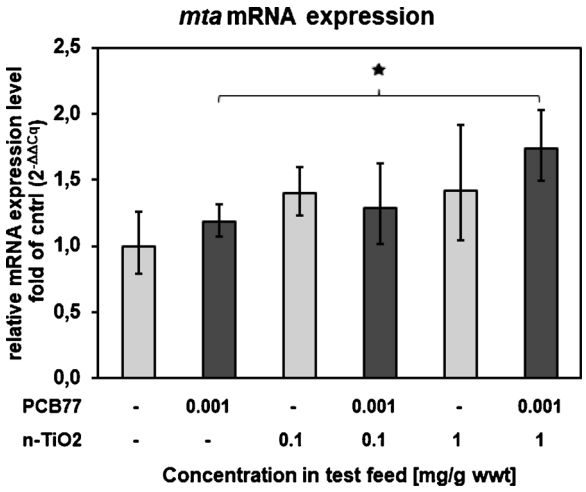

Fig. 5. Relative metallothionein mRNA expression levels in liver of brown trout receiving test diet spiked with n-TiO2, PCB77or n-TiO2 + PCB77. Bars and error bars show the mean fold change in gene expression level with respect to the negative control (-/-) and the lower/upper bound calculated from the standard error (SE) of $\Delta\Delta C_q$ values, respectively (n = 8). No statistically significant differences were observed in all pairwise comparisons (ANOVA). Significant differences detected comparing two treatment groups with each other are indicated by asterisks (*p < 0.05, *t*-test).

3.4.4. Correlation between hepatic biomarker response and measured PCB77 concentration

For the ten fish for which hepatic PCB77 concentrations were above the MDL a Spearman Rank Order Correlation analysis was conducted. The results showed no noteworthy correlation between the hepatic biomarker responses and PCB77 concentrations measured in each individual fish, except for GR. A moderate positive correlation was found between the ΔCq(*gr*)-values and PCB77 concentrations (r = 0.467, p = 0.160, n = 10) (Note that higher ΔCq-values indicate lower mRNA levels). Furthermore, in consistency with this result, a moderate negative correlation was identified between hepatic GR enzyme activities and PCB77 concentrations in each fish (r = -0.418, p = 0.213, n = 10). However, as indicated by the given p-values, there were no statistically significant relationships between the assessed variable pairs. Besides, no treatment-specific clusters could be observed when the GR mRNA and enzyme activity data were plotted against the measured PCB77 concentrations (data not shown). For EROD activities, on the other hand, although no significant overall correlation with hepatic PCB77 concentrations was found, treatment-specific data seemed to cluster when plotted in form of a multiple scatter plot (Figure A. 5).

4. Discussion

Manufactured nanomaterials, which are released into the aquatic environment, can interact and form complexes with organic chemical environmental pollutants and be taken up together or accumulate separately from each other in aquatic biota. Consequently, organisms,

Table 2
PCB77 concentrations in liver of brown trout receiving test diet spiked with n-TiO_2, PCB77, and n-TiO_2 + PCB77.

	Nominal dietborne dose [µg per day g ww fish]		
PCB77	0.01	0.01	0.01
n-TiO_2	–	1	10
Replicate/fish	Measured PCB77 concentration in liver [ng/g ww liver]		
1	0.035	0.032	< MDL
2	0.017	0.021	0.031
3	< MDL	< MDL	< MDL
4	< MDL	0.036	0.054
5	< MDL	< MDL	0.053
6	< MDL	< MDL	< MDL
7	< MDL	NA	< MDL
8	< MDL	0.032	0.026
mean	0.026	0.030	0.041
SD	± 0.009	± 0.006	± 0.013

which are higher up in the aquatic food chain such as fish, may be exposed to mixtures of manufactured nanomaterials and organic chemical environmental pollutants via the diet. In this study, we examined if and how simultaneous dietary exposure to n-TiO_2 and PCB77 influences their fate and effect in juvenile brown trout. We gave emphasis to the analysis of 1) intestine, as it is the first site of interaction and important barrier for dietary toxicants, and 2) liver, as it is one of the key organs concerning xenobiotic accumulation and detoxification. In both organs we found indications for combined toxicological effects, which are critically discussed below taking into account recognized and postulated modes of action of n-TiO_2 and PCBs.

4.1. Combined toxicological effects on intestine

We observed that *zo-1* transcript levels in intestinal tissue remained unaltered in the PCB77-only exposure (concentration in diet: 1 µg/g ww food; dietary dose: 10 ng/g fish ww/day; total dose: 150 ng/g fish ww), but increased significantly when n-TiO_2 was simultaneously present in the test diet (at a concentration of 1 mg/g ww food). Furthermore, exposure to n-TiO_2 alone at a dietary dose of 10 mg/kg bw/day did not have any effect on intestinal *zo-1* expression. This suggests that n-TiO_2 and PCB77 –or the molecular/cellular processes induced by them– interacted in a manner that led to a synergistic effect on this endpoint. This interpretation seems plausible because n-TiO_2 and PCBs were both shown to adversely affect tight junction integrity (Brun et al., 2014; Chen et al., 2016; Choi et al., 2010; Garcia-Rodriguez et al., 2018; Guo et al., 2017). For instance, tight junction protein expression in the small intestine of mice was found to be affected after a single gavage of 12.5 µg n-TiO_2 /g bw (Brun et al., 2014), and 150 nmol PCB/g bw (˜50 µg/g) (Choi et al., 2010). Thus, it is possible that a transcriptional response was triggered in the n-TiO_2/PCB mixture exposure because of a concerted effect exceeding a threshold level, which is not reached in the corresponding single substance exposures. Most previous studies concur in the finding that tight junction disruption following exposure to PCB or n-TiO_2 was related with a decrease in tight junction protein levels, but observations with respect to the effect at the transcriptional level differ (Brun et al., 2014; Cai et al., 2013; Choi et al., 2010; Eum et al., 2008; Guo et al., 2017; Seelbach et al., 2010; Selvakumar et al., 2013). For instance, Brun et al (2014) observed that intestinal n-TiO_2 exposure significantly increased epithelial permeability for FITC-Dextran (4 kDa), but mRNA levels of *zo-1* were ˜1.5-fold elevated compared to the control. We hypothesize that *zo-1* upregulation observed in the mixture exposure may reflect an adaptive response (i.e., compensatory tight junction protein synthesis) aiming at maintaining or restoring tight junction integrity.

The molecular processes underlying tight junction disruption are not yet fully understood, but literature suggests a relationship between intestinal tight junction dysregulation and oxidative stress (Chen et al., 2015; Choi et al., 2010; Guo et al., 2017; Maeda et al., 2010; Musch et al., 2006; Rao et al., 1997). Signs for perturbation of cellular redox homeostasis were also found in our study. For instance, PCB77 exposure appeared to result in slightly increased *sod-1* expression in the intestine, which may reflect a response to elevated reactive oxygen species (ROS) levels. This interpretation is consistent with literature showing that some PCBs including PCB77 can stimulate ROS production due to uncoupling of CYP1A (Schlezinger et al., 2006, 1999), which was expressed at high levels in the above fish. Besides, PCBs can promote ROS formation by activation of NAD(P)H oxidase (Choi et al., 2010; Myhre et al., 2009).

Dietary n-TiO_2 exposure did not have any effect on *sod-1* expression in our study. However, it resulted in altered transcript levels of the glutathione-related genes *gr* and *gpx*. While *gr* expression was significantly upregulated in n-TiO_2 only exposures (compared to control fish), *gpx* transcription appeared to be slightly suppressed in all n-TiO_2 containing treatments. Although GR enzyme activity was not affected by n-TiO_2, it is possible that n-TiO_2 caused a low level of oxidative stress and/or slightly compromised the tissue's antioxidant capacity rendering it more susceptible to PCB-induced effects resulting in enhanced ROS production. This could be a mechanistic explanation for the significant increase in *sod-1* and *zo-1* expression in the mixture exposure compared to the single substance exposures.

4.2. Combined toxicological effects on liver

Fish in the mixture treatment had higher hepatic *cyp1a* mRNA expression and CYP1A enzyme activity levels than fish exposed to PCB77 alone. The n-TiO_2 concentration-dependent trend and the statistically significant differences observed suggest a combined effect of both contaminants (i.e., n-TiO_2 and PCB77) on this endpoint. The fact that the measured effect levels in the mixture treatment were higher than the sum of the effect levels in the single substance treatment further suggests a synergetic interaction. Interestingly, exposure to n-TiO_2 alone also resulted in a small yet statistically significant increase in *cyp1a* transcription (compared to control fish). This is unexpected as the regulatory transcription factor, the aryl hydrocarbon receptor (AhR), is unlikely to be activated by a particulate contaminant. Yet, this observation is consistent with previous literature reporting upregulation of *cyp1a* in rat kidney following intragastric n-TiO_2 exposure (Gui et al., 2011) and in human lung fibroblasts in vitro (Periasamy et al., 2015). A possible explanation for this finding may be cross-talk activation of *cyp1a* transcription by the oxidative stress-induced Nrf-2/ARE signaling pathway (Gui et al., 2011; Periasamy et al., 2015; Shin et al., 2007). However, it must be noted that in this study n-TiO_2-induced *cyp1a* expression did not manifest at the enzyme activity level.

The reason behind the apparent potentiation of PCB77-induced EROD activity by n-TiO_2 remains to be elucidated. It is probable that the simultaneous presence of n-TiO_2 in the diet may have had some influence on the availability and intestinal uptake of the chemical. In this study, PCB77 was first spiked into the n-TiO_2 dispersion. Subsequently, the resulting mixture was added to the food. Thus, the chemical compound had occasion to bind to the NP surface. As a consequence its availability may be reduced. This hypothesis is supported by the fact that the amount of PCB77 that could be recovered during organic solvent extraction was inversely correlated to the n-TiO_2 concentration in the diet (see 3.1). However, the PCB77 concentration measured in liver suggests the opposite, namely that co-exposure to n-TiO_2 resulted in increased availability, uptake and hepatic accumulation of PCB77, which is also consistent with our observations at the effect level.

There are different possibilities for how n-TiO_2 might increase PCB availability, uptake or accumulation. For instance, the presence of high n-TiO_2 concentrations may increase the gut retention time resulting in more extended PCB77 exposure. Furthermore, the presence of NPs may have an influence on the interaction of PCBs with other components in the food/chyme such as lipids that affect the latter's solubility/bioavailability (Doi et al., 2000). It has also been suggested that the interaction of POPs with the catalytical nanosurface can result in their chemical transformation making them more water-soluble, and influence uptake and intra-organismal transport and distribution (Schon et al., 2017). In addition, the presence of n-TiO_2 may facilitate paracellular translocation of PCBs by impairing intestinal epithelial barrier function, for instance, due to oxidative stress-induced tight junction dysregulation. Another explanation may be that co-exposure to n-TiO_2 affects the metabolic degradation and elimination of PCB77, either directly by binding the chemical to their surface making it inaccessible for xenobiotic metabolizing enzymes, or indirectly by exerting additional stress on liver affecting the organs overall metabolic capacity. Moreover, it has been postulated that POPs can "hitchhike" on the surface of nanomaterials into organisms and accumulate in inner organs (Schon et al., 2017), for which we found, however, only limited evidence in this study.

The strong morphological resemblance of the electron-dense object

identified in TEM images of liver sections with the n-TiO_2 agglomerates present in the stock dispersion used for test diet spiking suggests that the imaged object is the nanomaterial tested in this study (please see appendix for further discussion). However, ICP-MS analysis showed that the Ti content in liver of n-TiO_2-exposed fish was not different from the blank (control fish) suggesting that there was no or no noteworthy accumulation in this organ following dietary exposure. However, the lack of supporting evidence does not invalidate our observation made by TEM. The presence/accumulation of n-TiO_2 in liver of fish (rainbow trout) has been shown before –including after dietary exposure (Ramsden et al., 2009; Scown et al., 2009). Although our observation should be interpreted with caution, it would be the first time that n-TiO_2 has been *imaged* in fish liver providing valuable information on the possible inner-organ distribution of the nanomaterial. The fact that the object was identified in the Space of Disse suggests that n-TiO_2 is taken up via the diet, enters the circulatory system, and can cross interior biological barriers insurmountable by larger particles, such as the fenestrated endothelium of liver sinusoids, which has an upper size cut-off between 75–120 nm (in rainbow trout) (Braet and Wisse, 2002). Consequently, n-TiO_2 may come in direct contact and interact with liver parenchymal cells/hepatocytes. During our TEM analysis we did not find any n-TiO_2 inside hepatocytes, but we previously demonstrated that n-TiO_2 agglomerates 30–100 nm in diameter can be endocytosed and accumulate in rainbow trout liver cells (RTL-W1) (Lammel et al., 2019).

Some support for n-TiO_2 uptake into liver cells may be given by the elevated hepatic *mta* mRNA levels measured in fish fed n-TiO_2-containing diet. However, there is only few evidence in the scientific literature that metallothionein can be induced by Ti (D'Agata et al., 2014; Sureda et al., 2018). Interestingly, hepatic metallothionein mRNA levels were higher in fish, which were fed diet containing both n-TiO_2 and PCB77 (1 and 0.001 mg/g food ww, respectively) compared to fish receiving diet containing only n-TiO_2. Although the difference was not significantly different in statistical terms, it may be indicative of a combined effect. There is increasing evidence that dioxin-like compounds can induce metallothionein expression (Fletcher et al., 2005; Frueh et al., 2001; Kurachi et al., 2002; Nishimura et al., 2001), possibly via crosstalk between the AhR and glucocorticoid receptor-mediated pathway (Sato et al., 2013).

5. Conclusions

This study demonstrates that dietary exposure of fish to n-TiO_2-PCB77-mixtures can result in effects that are larger than caused by dietary exposure to either of the two substances alone. For instance, genes encoding for proteins/enzymes vital for tight junction function (*zo-1*) and ROS elimination (*sod-1*) were significantly upregulated in intestinal tissue of fish receiving food co-contaminated with n-TiO_2 and PCB77, while no significant effect on these parameters was observed in the corresponding single-substance treatments. Also, the simultaneous presence of n-TiO_2 in the food had a potentiating effect on PCB77-induced biochemical responses in the liver, such as CYP1A and GR expression/enzyme activity. Both n-TiO_2-dependent changes in PCB77 availability, uptake and accumulation as well as concerted effects on shared endpoints could be the reason for the observed mixture effects. We identified an electron-dense object inside the Space of Disse of a liver sinusoid. The strong resemblance of this object with the n-TiO_2 incorporated into the diet suggests that the nanomaterial can cross both the intestinal epithelium and the fenestrated endothelium of liver sinusoids. However, ICP-MS data showed that there was no Ti accumulation in hepatic tissue. Therefore, it is unlikely that n-TiO_2 facilitated PCB77 transport and accumulation in liver by acting as a vector. Additional studies are needed to elucidate the complex toxicokinetic and toxicodynamic interactions of nanomaterials and organic chemical co-contaminants.

Conflict of interest

The author declare no conflict of interest.

Acknowledgments

The study and TL received financial support from the German Research Foundation (Deutsche Forschungsgemeinschaft, DFG) (Project number: 276093679) and the Swedish Research Council for Environment, Agricultural Sciences and Spatial Planning (FORMAS) (MENACE project; Grant reference number: 2016-00742). Furthermore, the authors acknowledge the Centre for Cellular Imaging (CCI) at the University of Gothenburg and the National Microscopy Infrastructure, NMI (VR-RFI 2016-00968) for providing assistance in microscopy, Dr. Stefan Gustafsson from the Chalmers Materials Analysis Laboratory for his help with EDX analysis of ultrathin sections of liver samples, Astrid Mikaelsson for her help counting blood cells, as well as Dr. Matthew MacLeod from the Department of Environmental Sciences and Analytical Chemistry; Stockholm University for facilitating access to and use of GC–MS instrumentation.

Appendix A. Supplementary data

Supplementary material related to this article can be found, in the online version, at doi:https://doi.org/10.1016/j.aquatox.2019.04.021.

References

Aebi, H., 1984. Catalase in vitro. Meth. Enzymol. 105, 121–126.
Al-Jubory, A.R., Handy, R.D., 2013. Uptake of titanium from TiO2 nanoparticle exposure in the isolated perfused intestine of rainbow trout: nystatin, vanadate and novel CO2-sensitive components. Nanotoxicology 7, 1282–1301.
Asztemborska, M., Jakubiak, M., Stęborowski, R., Chajduk, E., Bystrzejewska-Piotrowska, G., 2018. Titanium dioxide nanoparticle circulation in an aquatic ecosystem. Water Air Soil Pollut. 229, 208.
Bigorgne, E., Foucaud, L., Lapied, E., Labile, J., Botta, C., Sirguey, C., Falla, J., Rose, J., Joner, E.J., Rodius, F., Nahmani, J., 2011. Ecotoxicological assessment of TiO2 by-products on the earthworm Eisenia fetida. Environ. Pollut. 159, 2698–2705.
Boxall, A., Chaudhry, Q., Sinclair, C., Jones, A., Aitken, R., Jefferson, B., Watts, C., 2007. Current and Future Predicted Environmental Exposure to Engineered Nanoparticles. Central Science Laboratory, Department of the Environment and Rural Affairs, London, UK Accessed October 2014. http://hero.epa.gov/index.cfm?action=search.view&reference_id=196111.
Braet, F., Wisse, E., 2002. Structural and functional aspects of liver sinusoidal endothelial cell fenestrae: a review. Comp. Hepatol. 1, 1.
Brun, E., Barreau, F., Veronesi, G., Fayard, B., Sorieul, S., Chaneac, C., Carapito, C., Rabilloud, T., Mabondzo, A., Herlin-Boime, N., Carriere, M., 2014. Titanium dioxide nanoparticle impact and translocation through ex vivo, in vivo and in vitro gut epithelia. Part. Fibre Toxicol. 11.
Brunelli, A., Pojana, G., Callegaro, S., Marcomini, A., 2013. Agglomeration and sedimentation of titanium dioxide nanoparticles (n-TiO2) in synthetic and real waters. J. Nanopart. Res. 15, 10.
Cai, J.L., Wang, C.G., Huang, L.X., Chen, M., Zuo, Z.H., 2013. A novel effect of polychlorinated biphenyls: impairment of the tight junctions in the mouse epididymis. Toxicol. Sci. 134, 382–390.
Canesi, L., Ciacci, C., Balbi, T., 2015. Interactive effects of nanoparticles with other contaminants in aquatic organisms: friend or foe? Mar. Environ. Res. 111, 128–134.
Canesi, L., Frenzilli, G., Balbi, T., Bernardeschi, M., Ciacci, C., Corsolini, S., Della Torre, C., Fabbri, R., Faleri, C., Focardi, S., Guidi, P., Kocan, A., Marcomini, A., Mariottini, M., Nigro, M., Pozo-Gallardo, K., Rocco, L., Scarcelli, V., Smerilli, A., Corsi, I., 2014. Interactive effects of n-TiO2 and 2,3,7,8-TCDD on the marine bivalve Mytilus galloprovincialis. Aquat. Toxicol. 153, 53–65.
Chen, I.C., Hsiao, I.L., Lin, H.C., Wu, C.H., Chuang, C.Y., Huang, Y.J., 2016. Influence of silver and titanium dioxide nanoparticles on in vitro blood-brain barrier permeability. Environ. Toxicol. Pharmacol. 47, 108–118.
Chen, L., Feng, L., Jiang, W.-D., Jiang, J., Wu, P., Zhao, J., Kuang, S.-Y., Tang, L., Tang, W.-N., Zhang, Y.-A., Zhou, X.-Q., Liu, Y., 2015. Intestinal immune function, antioxidant status and tight junction proteins mRNA expression in young grass carp (Ctenopharyngodon idella) fed riboflavin deficient diet. Fish Shellfish Immunol. 47, 470–484.
Chen, L.G., Guo, Y.Y., Hu, C.Y., Lam, P.K.S., Lam, J.C.W., Zhou, B.S., 2018. Dysbiosis of gut microbiota by chronic coexposure to titanium dioxide nanoparticles and bisphenol A: implications for host health in zebrafish. Environ. Pollut. 234, 307–317.
Chen, L.G., Hu, C.Y., Guo, Y.Y., Shi, Q.P., Zhou, B.S., 2019. TiO2 nanoparticles and BPA are combined to impair the development of offspring zebrafish after parental coexposure. Chemosphere 217, 732–741.
Choi, Y.J., Seelbach, M.J., Pu, H., Eum, S.Y., Chen, L., Zhang, B., Hennig, B., Toborek, M.,

2010. Polychlorinated biphenyls disrupt intestinal integrity via NADPH oxidase-induced alterations of tight junction protein expression. Environ. Health Perspect. 118, 976–981.
Coll, C., Notter, D., Gottschalk, F., Sun, T., Som, C., Nowack, B., 2016. Probabilistic environmental risk assessment of five nanomaterials (nano-TiO2, nano-Ag, nano-ZnO, CNT, and fullerenes). Nanotoxicology 10, 436–444.
Cribb, A.E., Leeder, J.S., Spielberg, S.P., 1989. Use of a microplate reader in an assay of glutathione-reductase using 5,5′-dithiobis(2-nitrobenzoic acid). Anal. Biochem. 183, 195–196.
Ctistis, G., Schon, P., Bakker, W., Luthe, G., 2016. PCDDs, PCDFs, and PCBs co-occurrence in TiO2 nanoparticles. Environ. Sci. Pollut. Res. 23, 4837–4843.
D'Agata, A., Fasulo, S., Dallas, L.J., Fisher, A.S., Maisano, M., Readman, J.W., Jha, A.N., 2014. Enhanced toxicity of' bulk' titanium dioxide compared to' fresh' and' aged' nano-TiO2 in marine mussels (Mytilus galloprovincialis). Nanotoxicology 8, 549–558.
Della Torre, C., Buonocore, F., Frenzilli, G., Corsolini, S., Brunelli, A., Guidi, P., Kocan, A., Mariottini, M., Mottola, F., Nigro, M., Pozo, K., Randelli, E., Vannuccini, M.L., Picchietti, S., Santonastaso, M., Scarcelli, V., Focardi, S., Marcomini, A., Rocco, L., Scapigliati, G., Corsi, I., 2015. Influence of titanium dioxide nanoparticles on 2,3,7,8-tetrachlorodibenzo-p-dioxin bioconcentration and toxicity in the marine fish European sea bass (Dicentrarchus labrax). Environ. Pollut. 196, 185–193.
Doi, A.M., Lou, Z., Holmes, E., Li, C.L.J., Venugopal, C.S., James, M.O., Kleinow, K.M., 2000. Effect of Micelle Fatty Acid Composition and 3,4,3′,4′-Tetrachlorobiphenyl (TCB) Exposure on Intestinal [14C]-TCB Bioavailability and Biotransformation in Channel Catfish in Situ Preparations. Toxicol. Sci. 55, 85–96.
Eum, S.Y., András, I.E., Couraud, P.-O., Hennig, B., Toborek, M., 2008. PCBs and tight junction expression. Environ. Toxicol. Pharmacol. 25, 234–240.
Fang, Q., Shi, Q.P., Guo, Y.Y., Hua, J.H., Wang, X.F., Zhou, B.S., 2016. Enhanced bioconcentration of bisphenol A in the presence of Nano-TiO2 can lead to adverse reproductive outcomes in zebrafish. Environ. Sci. Technol. 50, 1005–1013.
Federici, G., Shaw, B.J., Handy, R.D., 2007. Toxicity of titanium dioxide nanoparticles to rainbow trout (Oncorhynchus mykiss): gill injury, oxidative stress, and other physiological effects. Aquat. Toxicol. 84, 415–430.
Fletcher, N., Wahlström, D., Lundberg, R., Nilsson, C.B., Nilsson, K.C., Stockling, K., Hellmold, H., Håkansson, H., 2005. 2,3,7,8-Tetrachlorodibenzo-p-dioxin (TCDD) alters the mRNA expression of critical genes associated with cholesterol metabolism, bile acid biosynthesis, and bile transport in rat liver: a microarray study. Toxicol. Appl. Pharmacol. 207, 1–24.
Forlin, L., Andersson, T., Koivusaari, U., Hansson, T., 1984. Influence of biological and environmental-factors on hepatic-steroid and xenobiotic metabolism in fish - interaction with Pcb and beta-naphthoflavone. Mar. Environ. Res. 14, 47–58.
Frueh, F.W., Hayashibara, K.C., Brown, P.O., Whitlock, J.P., 2001. Use of cDNA microarrays to analyze dioxin-induced changes in human liver gene expression. Toxicol. Lett. 122, 189–203.
Galloway, T., Lewis, C., Dolciotti, I., Johnston, B.D., Moger, J., Regoli, F., 2010. Sublethal toxicity of nano-titanium dioxide and carbon nanotubes in a sediment dwelling marine polychaete. Environ. Pollut. 158, 1748–1755.
Garcia-Rodriguez, A., Vila, L., Cortes, C., Hernandez, A., Marcos, R., 2018. Effects of differently shaped TiO(2)NPs (nanospheres, nanorods and nanowires) on the in vitro model (Caco-2/HT29) of the intestinal barrier. Part. Fibre Toxicol. 15, 16.
Gondikas, A., von der Kammer, F., Kaegi, R., Borovinskaya, O., Neubauer, E., Navratilova, J., Praetorius, A., Cornelis, G., Hofmann, T., 2018. Where is the nano? Analytical approaches for the detection and quantification of TiO2 engineered nanoparticles in surface waters. Environ. Sci. Nano 5, 313–326.
Gottschalk, F., Ort, C., Scholz, R.W., Nowack, B., 2011. Engineered nanomaterials in rivers - exposure scenarios for Switzerland at high spatial and temporal resolution. Environ. Pollut. 159, 3439–3445.
Gottschalk, F., Sonderer, T., Scholz, R.W., Nowack, B., 2009. Modeled environmental concentrations of engineered nanomaterials (TiO2, ZnO, Ag, CNT, Fullerenes) for different regions. Environ. Sci. Technol. 43, 9216–9222.
Gui, S., Zhang, Z., Zheng, L., Cui, Y., Liu, X., Li, N., Sang, X., Sun, Q., Gao, G., Cheng, Z., Cheng, J., Wang, L., Tang, M., Hong, F., 2011. Molecular mechanism of kidney injury of mice caused by exposure to titanium dioxide nanoparticles. J. Hazard. Mater. 195, 365–370.
Guo, Y.Y., Chen, L.G., Wu, J., Hua, J.H., Yang, L.H., Wang, Q.W., Zhang, W., Lee, J.S., Zhou, B.S., 2019. Parental co-exposure to bisphenol A and nano-TiO2 causes thyroid endocrine disruption and developmental neurotoxicity in zebrafish offspring. Sci. Total Environ. 650, 557–565.
Guo, Z.Y., Martucci, N.J., Moreno-Olivas, F., Tako, E., Mahler, G.J., 2017. Titanium dioxide nanoparticle ingestion alters nutrient absorption in an in vitro model of the small intestine. Nano Impact 5, 70–82.
Habig, W.H., Pabst, M.J., Jakoby, W.B., 1974. Glutathione S-transferases - first enzymatic step in mercapturic acid formation. J. Biol. Chem. 249, 7130–7139.
Hansen, B.H., Garmo, O.A., Olsvik, P.A., Andersen, R.A., 2007a. Gill metal binding and stress gene transcription in brown trout (Salmo trutta) exposed to metal environments: the effect of pre-exposure in natural populations. Environ. Toxicol. Chem. 26, 944–953.
Hansen, B.H., Romma, S., Garmo, O.A., Pedersen, S.A., Olsvik, P.A., Andersen, R.A., 2007b. Induction and activity of oxidative stress-related proteins during waterborne Cd/Zn-exposure in brown trout (Salmo trutta). Chemosphere 67, 2241–2249.
Hansen, S.F., Heggelund, L.R., Besora, P.R., Mackevica, A., Boldrin, A., Baun, A., 2016. Nanoproducts - what is actually available to European consumers? Environ. Sci. Nano 3, 169–180.
Hartmann, N.B., Baun, A., 2010. The nano cocktail: ecotoxicological effects of engineered nanoparticles in chemical mixtures. Integr. Environ. Assess. Manag. 6, 311–313.
Hartmann, N.B., Legros, S., Von der Kammer, F., Hofmann, T., Baun, A., 2012. The potential of TiO2 nanoparticles as carriers for cadmium uptake in Lumbriculus variegatus and Daphnia magna. Aquat. Toxicol. 118, 1–8.
Hu, C.W., Li, M., Cui, Y.B., Li, D.S., Chen, J., Yang, L.Y., 2010. Toxicological effects of TiO2 and ZnO nanoparticles in soil on earthworm Eisenia fetida. Soil Biol. Biochem. 42, 586–591.
Jhamtani, R.C., Shukla, S., Sivaperumal, P., Dahiya, M.S., Agarwal, R., 2018. Impact of co-exposure of aldrin and titanium dioxide nanoparticles at biochemical and molecular levels in Zebrafish. Environ. Toxicol. Pharmacol. 58, 141–155.
Johnson, A.C., Bowes, M.J., Crossley, A., Jarvie, H.P., Jurkschat, K., Jürgens, M.D., Lawlor, A.J., Park, B., Rowland, P., Spurgeon, D., Svendsen, C., Thompson, I.P., Barnes, R.J., Williams, R.J., Xu, N., 2011. An assessment of the fate, behaviour and environmental risk associated with sunscreen TiO2 nanoparticles in UK field scenarios. Sci. Total Environ. 409, 2503–2510.
Kaegi, R., Ulrich, A., Sinnet, B., Vonbank, R., Wichser, A., Zuleeg, S., Simmler, H., Brunner, S., Vonmont, H., Burkhardt, M., Boller, M., 2008. Synthetic TiO(2) nanoparticle emission from exterior facades into the aquatic environment. Environ. Pollut. 156, 233–239.
Kaida, T., Kobayashi, K., Adachi, M., Suzuki, F., 2004. Optical characteristics of titanium oxide interference film and the film laminated with oxides and their applications for cosmetics. J. Cosmet. Sci. 55, 219–220.
Kelly, S.P., Chasiotis, H., 2011. Glucocorticoid and mineralocorticoid receptors regulate paracellular permeability in a primary cultured gill epithelium. J. Exp. Biol. 214, 2308–2318.
Kim, J.I., Park, H.G., Chang, K.H., Nam, D.H., Yeo, M.K., 2016. Trophic transfer of nano-TiO2 in a paddy microcosm: a comparison of single-dose versus sequential multi-dose exposures. Environ. Pollut. 212, 316–324.
Kurachi, M., Hashimoto, S.-i., Obata, A., Nagai, S., Nagahata, T., Inadera, H., Sone, H., Tohyama, C., Kaneko, S., Kobayashi, K.-i., Matsushima, K., 2002. Identification of 2,3,7,8-Tetrachlorodibenzo-p-dioxin-responsive genes in mouse liver by serial analysis of gene expression. Biochem. Biophys. Res. Commun. 292, 368–377.
Lammel, T., Mackevica, A., Johansson, B.R., J, S, 2019. Endocytosis, intracellular fate, accumulation and agglomeration of titanium dioxide (TiO2) nanoparticles in the rainbow trout liver cell line RTL-W1. Environ. Sci. Pollut. Res In Press.
Lammel, T., Sturve, J., 2018. Assessment of titanium dioxide nanoparticle toxicity in the rainbow trout (Onchorynchus mykiss) liver and gill cell lines RTL-W1 and RTgill-W1 under particular consideration of nanoparticle stability and interference with fluorometric assays. NanoImpact 11, 1–19.
Lapied, E., Nahmani, J.Y., Moudilou, E., Chaurand, P., Labille, J., Rose, J., Exbrayat, J.-M., Oughton, D.H., Joner, E.J., 2011. Ecotoxicological effects of an aged TiO2 nanocomposite measured as apoptosis in the anecic earthworm Lumbricus terrestris after exposure through water, food and soil. Environ. Int. 37, 1105–1110.
Li, S., Wallis, L.K., Ma, H., Diamond, S.A., 2014. Phototoxicity of TiO2 nanoparticles to a freshwater benthic amphipod: are benthic systems at risk? Sci. Total Environ. 466-467, 800–808.
Lowry, O.H., Rosebrough, N.J., Farr, A.L., Randall, R.J., 1951. Protein measurement with the Folin phenol reagent. J. Biol. Chem. 193, 265–275.
Maeda, T., Miyazono, Y., Ito, K., Hamada, K., Sekine, S., Horie, T., 2010. Oxidative stress and enhanced paracellular permeability in the small intestine of methotrexate-treated rats. Cancer Chemother. Pharmacol. 65, 1117–1123.
Marabini, L., Calo, R., Fucile, S., 2011. Genotoxic effects of polychlorinated biphenyls (PCB 153, 138, 101, 118) in a fish cell line (RTG-2). Toxicol. In Vitro 25, 1045–1052.
Maruya, K.A., Lee, R.E., 1998. Biota-sediment accumulation and trophic transfer factors for extremely hydrophobic polychlorinated biphenyls. Environ. Toxicol. Chem. 17, 2463–2469.
Meland, S., Heier, L.S., Salbu, B., Tollefsen, K.E., Farmen, E., Rosseland, B.O., 2010. Exposure of brown trout (Salmo trutta L.) to tunnel wash water runoff - Chemical characterisation and biological impact. Sci. Total Environ. 408, 2646–2656.
Menard, A., Drobne, D., Jemec, A., 2011. Ecotoxicity of nanosized TiO2. Review of in vivo data. Environ. Pollut. 159, 677–684.
Moermond, C.T.A., Roozen, F., Zwolsman, J.J.G., Koelmans, A.A., 2004. Uptake of sediment-bound bioavailable polychlorobiphenyls by benthivorous carp (Cyprinus carpio). Environ. Sci. Technol. 38, 4503–4509.
Musch, M.W., Walsh-Reitz, M.M., Chang, E.B., 2006. Roles of ZO-1, occludin, and actin in oxidant-induced barrier disruption. Am. J. Physiol. Gastrointest. Liver Physiol. 290, G222–G231.
Myhre, O., Mariussen, E., Reistad, T., Voie, O.A., Aarnes, H., Fonnum, F., 2009. Effects of polychlorinated biphenyls on the neutrophil NADPH oxidase system. Toxicol. Lett. 187, 144–148.
Naasz, S., Altenburger, R., Kühnel, D., 2018. Environmental mixtures of nanomaterials and chemicals: the Trojan-horse phenomenon and its relevance for ecotoxicity. Sci. Total Environ. 635, 1170–1181.
Nishimura, N., Miyabara, Y., Suzuki, J.S., Sato, M., Aoki, Y., Satoh, M., Yonemoto, J., Tohyama, C., 2001. Induction of metallothionein in the livers of female Sprague-Dawley rats treated with 2,3,7,8-tetrachlorodibenzo-p-dioxin. Life Sci. 69, 1291–1303.
Pena-Abaurrea, M., de la Torre, V.S.G., Ramos, L., 2013. Ultrasound-assisted extraction followed by disposable pipette purification for the determination of polychlorinated biphenyls in small-size biological tissue samples. J. Chromatogr. A 1317, 223–229.
Periasamy, V.S., Athinarayanan, J., Al-Hadi, A.M., Juhaimi, F.A., Mahmoud, M.H., Alshatwi, A.A., 2015. Identification of titanium dioxide nanoparticles in food products: induce intracellular oxidative stress mediated by TNF and CYP1A genes in human lung fibroblast cells. Environ. Toxicol. Pharmacol. 39, 176–186.
Peters, R.J.B., van Bemmel, G., Milani, N.B.L., den Hertog, G.C.T., Undas, A.K., van der Lee, M., Bouwmeester, H., 2018. Detection of nanoparticles in Dutch surface waters. Sci. Total Environ. 621, 210–218.
Piccinno, F., Gottschalk, F., Seeger, S., Nowack, B., 2012. Industrial production quantities

and uses of ten engineered nanomaterials in Europe and the world. J. Nanopart. Res. 14, 11.
Praetorius, A., Scheringer, M., Hungerbühler, K., 2012. Development of environmental fate models for engineered nanoparticles—a case study of TiO2 nanoparticles in the Rhine river. Environ. Sci. Technol. 46, 6705–6713.
Qiang, L.W., Pan, X.Y., Zhu, L.Y., Fang, S.H., Tian, S.Y., 2016. Effects of nano-TiO2 on perfluorooctanesulfonate bioaccumulation in fishes living in different water layers: implications for enhanced risk of perfluorooctanesulfonate. Nanotoxicology 10, 471–479.
Ramsden, C.S., Smith, T.J., Shaw, B.J., Handy, R.D., 2009. Dietary exposure to titanium dioxide nanoparticles in rainbow trout, (Oncorhynchus mykiss): no effect on growth, but subtle biochemical disturbances in the brain. Ecotoxicology 18, 939–951.
Rao, R.K., Baker, R.D., Baker, S.S., Gupta, A., Holycross, M., 1997. Oxidant-induced disruption of intestinal epithelial barrier function: role of protein tyrosine phosphorylation. Am. J. Physiol. Gastrointest. Liver Physiol. 273, G812–G823.
Ren, X., Zhao, X.S., Duan, X.Y., Fang, Z.W., 2018. Enhanced bio-concentration of tris(1,3-dichloro-2-propyl) phosphate in the presence of nano-TiO2 can lead to adverse reproductive outcomes in zebrafish. Environ. Pollut. 233, 612–622.
Sato, S., Shirakawa, H., Tomita, S., Tohkin, M., Gonzalez, F.J., Komai, M., 2013. The aryl hydrocarbon receptor and glucocorticoid receptor interact to activate human metallothionein 2A. Toxicol. Appl. Pharmacol. 273, 90–99.
Schlezinger, J.J., Stegeman, J.J., 2001. Induction and suppression of cytochrome P450 1A by 3,3',4,4′,5-pentachlorobiphenyl and its relationship to oxidative stress in the marine fish scup (Stenotomus chrysops). Aquat. Toxicol. 52, 101–115.
Schlezinger, J.J., Struntz, W.D.J., Goldstone, J.V., Stegeman, J.J., 2006. Uncoupling of cytochrome P450 1A and stimulation of reactive oxygen species production by coplanar polychlorinated biphenyl congeners. Aquat. Toxicol. 77, 422–432.
Schlezinger, J.J., White, R.D., Stegeman, J.J., 1999. Oxidative inactivation of cytochrome P-450 1A (CYP1A) stimulated by 3,3',4,4′-tetrachlorobiphenyl: Production of reactive oxygen by vertebrate CYP1As. Mol. Pharmacol. 56, 588–597.
Schmid, K., Riediker, M., 2008. Use of nanoparticles in Swiss industry: a targeted survey. Environ. Sci. Technol. 42, 2253–2260.
Schon, P., Ctistis, G., Bakker, W., Luthe, G., 2017. Nanoparticular surface-bound PCBs, PCDDs, and PCDFs-a novel class of potentially higher toxic POPs. Environ. Sci. Pollut. Res. 24, 12758–12766.
Scown, T.M., van Aerle, R., Johnston, B.D., Cumberland, S., Lead, J.R., Owen, R., Tyler, C.R., 2009. High doses of intravenously administered titanium dioxide nanoparticles accumulate in the kidneys of rainbow trout but with no observable impairment of renal function. Toxicol. Sci. 109, 372–380.
Seelbach, M., Chen, L., Powell, A., Choi, Y.J., Zhang, B., Hennig, B., Toborek, M., 2010. Polychlorinated biphenyls disrupt blood-brain barrier integrity and promote brain metastasis formation. Environ. Health Perspect. 118, 479–484.
Selvakumar, K., Prabha, R.L., Saranya, K., Bavithra, S., Krishnamoorthy, G., Arunakaran, J., 2013. Polychlorinated biphenyls impair blood-brain barrier integrity via disruption of tight junction proteins in cerebrum, cerebellum and hippocampus of female Wistar rats: neuropotential role of quercetin. Hum. Exp. Toxicol. 32, 706–720.
Shi, H., Magaye, R., Castranova, V., Zhao, J., 2013. Titanium dioxide nanoparticles: a review of current toxicological data. Part. Fibre Toxicol. 10, 15.
Shi, Y., Zhang, J.-H., Jiang, M., Zhu, L.-H., Tan, H.-Q., Lu, B., 2010. Synergistic genotoxicity caused by low concentration of titanium dioxide nanoparticles and p,p' -DDT in human hepatocytes. Environ. Mol. Mutagen. 51, 192–204.
Shin, S., Wakabayashi, N., Misra, V., Biswal, S., Lee, G.H., Agoston, E.S., Yamamoto, M., Kensler, T.W., 2007. NRF2 modulates aryl hydrocarbon receptor signaling: influence on adipogenesis. Mol. Cell. Biol. 27, 7188–7197.
Slomberg, D.L., Ollivier, P., Miche, H., Angeletti, B., Bruchet, A., Philibert, M., Brant, J., Labille, J., 2019. Nanoparticle stability in lake water shaped by natural organic matter properties and presence of particulate matter. Sci. Total Environ. 656, 338–346.
Stephensen, E., Sturve, J., Forlin, L., 2002. Effects of redox cycling compounds on glutathione content and activity of glutathione-related enzymes in rainbow trout liver. Comp. Biochem. Physiol. C Toxicol. Pharmacol. 133, 435–442.
Sturve, J., Berglund, A., Balk, L., Broeg, K., Bohmert, B., Massey, S., Savva, D., Parkkonen, J., Stephensen, E., Koehler, A., Forlin, L., 2005. Effects of dredging in Goteborg Harbor, Sweden, assessed by biomarkers in eelpout (Zoarces viviparus). Environ. Toxicol. Chem. 24, 1951–1961.
Sun, T.Y., Gottschalk, F., Hungerbühler, K., Nowack, B., 2014. Comprehensive probabilistic modelling of environmental emissions of engineered nanomaterials. Environ. Pollut. 185, 69–76.
Sureda, A., Capó, X., Busquets-Cortés, C., Tejada, S., 2018. Acute exposure to sunscreen containing titanium induces an adaptive response and oxidative stress in Mytillus galloprovincialis. Ecotoxicol. Environ. Saf. 149, 58–63.
Van Geest, J.L., Mackay, D., Poirier, D.G., Sibley, P.K., Solomon, K.R., 2011. Accumulation and depuration of polychlorinated biphenyls from field-collected sediment in three freshwater organisms. Environ. Sci. Technol. 45, 7011–7018.
Vignardi, C.P., Hasue, F.M., Sartorio, P.V., Cardoso, C.M., Machado, A.S.D., Passos, M., Santos, T.C.A., Nucci, J.M., Hewer, T.L.R., Watanabe, I.S., Gomes, V., Phan, N.V., 2015. Genotoxicity, potential cytotoxicity and cell uptake of titanium dioxide nanoparticles in the marine fish Trachinotus carolinus (Linnaeus, 1766). Aquat. Toxicol. 158, 218–229.
Wang, Q.W., Chen, Q., Zhou, P., Li, W.W., Wang, J.X., Huang, C.J., Wang, X.F., Lin, K.F., Zhou, B.S., 2014. Bioconcentration and metabolism of BDE-209 in the presence of titanium dioxide nanoparticles and impact on the thyroid endocrine system and neuronal development in zebrafish larvae. Nanotoxicology 8, 196–207.
Wang, Z., Yin, L., Zhao, J., Xing, B., 2016. Trophic transfer and accumulation of TiO2 nanoparticles from clamworm (Perinereis aibuhitensis) to juvenile turbot (Scophthalmus maximus) along a marine benthic food chain. Water Res. 95, 250–259.
Yan, J., Lin, B., Hu, C., Zhang, H., Lin, Z., Xi, Z., 2014a. The combined toxicological effects of titanium dioxide nanoparticles and bisphenol A on zebrafish embryos. Nanoscale Res. Lett. 9, 406.
Yan, J., Lin, B.C., Hu, C.L., Zhang, H.S., Lin, Z.Q., Xi, Z.G., 2014b. The combined toxicological effects of titanium dioxide nanoparticles and bisphenol A on zebrafish embryos. Nanoscale Res. Lett. 9.
Yang, W.-W., Wang, Y., Huang, B., Wang, N.-X., Wei, Z.-B., Luo, J., Miao, A.-J., Yang, L.-Y., 2014. TiO2 nanoparticles act as a carrier of Cd bioaccumulation in the ciliate Tetrahymena thermophila. Environ. Sci. Technol. 48, 7568–7575.
Zhang, X., Sun, H., Zhang, Z., Niu, Q., Chen, Y., Crittenden, J.C., 2007. Enhanced bioaccumulation of cadmium in carp in the presence of titanium dioxide nanoparticles. Chemosphere 67, 160–166.
Zhu, X., Chang, Y., Chen, Y., 2010. Toxicity and bioaccumulation of TiO2 nanoparticle aggregates in Daphnia magna. Chemosphere 78, 209–215.